

Recombination Dynamics and Hydrogen Abstraction Reactions of Chlorine Radicals in Solution

Leonid Sheps, Andrew C. Crowther, Christopher G. Elles,[†] and F. Fleming Crim*

Department of Chemistry, University of Wisconsin, Madison, Wisconsin 53706

Received: March 2, 2005

We observe chlorine radical dynamics in solution following two-photon photolysis of the solvent, dichloromethane. In neat CH₂Cl₂, one-third of the chlorine radicals undergo diffusive geminate recombination, and the rest abstract a hydrogen atom from the solvent with a bimolecular rate constant of $(1.35 \pm 0.06) \times 10^7 \text{ M}^{-1} \text{ s}^{-1}$. Upon addition of hydrogen-containing solutes, the chlorine atom decay becomes faster, reflecting the presence of a new reaction pathway. We study 16 different solutes that include alkanes (pentane, hexane, heptane, and their cyclic analogues), alcohols (methanol, ethanol, 1-propanol, 2-propanol, and 1-butanol), and chlorinated alkanes (cyclohexyl chloride, 1-chlorobutane, 2-chlorobutane, 1,2-dichlorobutane, and 1,4-dichlorobutane). Chlorine reactions with alkanes have diffusion-limited rate constants that do not depend on the molecular structure, indicating the absence of a potential barrier. Hydrogen abstraction from alcohols is slower than from alkanes and depends weakly on molecular structure, consistent with a small reaction barrier. Reactions with chlorinated alkanes are the slowest, and their rate constants depend strongly on the number and position of the chlorine substituents, signaling the importance of activation barriers to these reactions. The relative rate constants for the activation-controlled reactions agree very well with the predictions of the gas-phase structure–activity relationships.

I. Introduction

Hydrogen abstraction by atomic chlorine is a model system for investigating the dynamics of bimolecular reactions in gases and liquids. In the gas phase, chlorine radical chemistry has received a great deal of attention because of its importance in the atmosphere, particularly with respect to ozone depletion.^{1–4} There are thorough studies covering a wide temperature range for reactions with small alkanes,^{5–7} alcohols,⁸ aldehydes,⁹ ethers,¹⁰ and their various halogenated derivatives.^{11–14} Well-developed gas-phase detection techniques can distinguish between different products and, thus, investigate the selectivity of chlorine attack. As a result, the temperature-dependent gas-phase rates of these reactions and their mechanisms are well-known, allowing experimental determination of bond strengths and activation energies for the abstraction of individual hydrogen atoms.^{5,6,12,14} These insights gleaned from gas-phase experiments form a basis for understanding reactions in liquids.

The gas-phase studies show persistent trends in the reactivity of small organic molecules toward chlorine atoms. Specifically, the activation energy for abstraction of a primary hydrogen is higher than that for secondary or tertiary hydrogens. In addition, the presence of halogen substituents generally raises the activation energy for abstraction of neighboring hydrogens. This effect increases with increasing electronegativity of the halogen and is stronger for β -hydrogens than that for α -hydrogens. These trends led to the idea of structure–activity relationships that predict the reactivity of a molecule toward chlorine from its structure.^{15,16} The relationships assign a reactivity to every hydrogen atom, based on its position (primary, secondary, or

tertiary) and weight it according to the identity of its neighboring groups. Summing all of the contributions gives the total reaction rate constant k_{total} of a molecule

$$k_{\text{total}} = \sum_{H_{\text{pri}}} k_{\text{pri}} F(X) + \sum_{H_{\text{sec}}} k_{\text{sec}} F(X)F(Y) + \sum_{H_{\text{ter}}} k_{\text{ter}} F(X)F(Y)F(Z) \quad (1)$$

where k_{pri} , k_{sec} , and k_{ter} are reaction rate constants for hydrogens in various positions and $F(X)$, $F(Y)$, $F(Z)$ are the weighting factors. Structure–activity relationships successfully predict hydrogen abstraction rates by chlorine atoms or by hydroxyl radicals from a variety of small molecules. The weighting factors for many common neighboring groups, such as methyl, ethyl, OH, and Cl, are available from fits to experimental results.^{15,16}

Experimental data on chlorine reactions in solution are more limited. Early microsecond or nanosecond time-resolved studies used absorption of visible wavelengths by a chlorine atom–arene or chlorine atom–DMSO complex to monitor chlorine radical populations in solutions of organic molecules.^{17–19} The investigators then inferred the reaction rates through complicated competitive reaction schemes. In a series of more direct experiments, Chateaufort assigned a transient ultraviolet absorption centered at 330 nm to the “free” chlorine atom in solutions of dichloromethane, chloroform, and several other molecules and showed that the hydrogen abstraction rates depend on the solvent.^{20,21} He suggested that atomic chlorine forms complexes with many common solvents and that the reactive species observed in solution is a chlorine–solvent complex rather than a free chlorine radical.²² Advances in time-resolved laser techniques have made it possible to measure even very fast reaction rates directly. For example, Raftery et al. used picosecond infrared probe pulses to monitor the evolution of

* Author to whom correspondence should be addressed. E-mail: fcgrim@chem.wisc.edu.

[†] Present addresses: Department of Chemistry, University of Southern California, Los Angeles, CA 90089, and Chemistry Division, Argonne National Laboratory, Argonne, IL 60439.

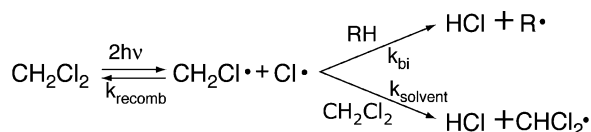


Figure 1. Reaction scheme following photodissociation of CH_2Cl_2 . The quantity $2h\nu$ is the two-photon photolysis with a 266-nm photolysis laser pulse, and k_{recomb} is diffusive geminate recombination. k_{bi} and k_{solvent} are the rate constants for hydrogen abstraction from the solute and the solvent, respectively.

the HCl product of hydrogen abstraction by chlorine in neat cyclohexane.²³ Keiding and co-workers reported two ultrafast studies of chlorine radical reactions produced by the photolysis of HOCl in water.^{24,25} Most recently, Elles et al. performed a thorough study of the photodissociation of CH_3OCl and of the subsequent chlorine dynamics in solution.²⁶

Here, we describe a femtosecond time-resolved pump–probe study of chlorine radical reactions in CH_2Cl_2 solutions of 16 different organic molecules. The solutes are alkanes (pentane, hexane, heptane, and their cyclic analogues), alcohols (methanol, ethanol, 1-propanol, 2-propanol, and 1-butanol), and chlorinated alkanes (cyclohexyl chloride, 1-chlorobutane, 2-chlorobutane, 1,2-dichlorobutane, and 1,4-dichlorobutane). We generate chlorine atoms by two-photon photolysis of the CH_2Cl_2 solvent with a 266-nm, 100-fs laser pulse. The chlorine radicals subsequently evolve according to the reaction scheme shown in Figure 1. Immediately after photolysis, we observe the chlorine radical by using its characteristic charge-transfer transition centered at about 330 nm. We tune a probe pulse to the maximum of this band and follow the temporal evolution of chlorine radicals in a range of concentrations of each solute. For all solute concentrations, the chlorine signal has a fast, nonexponential decay followed by a slow exponential decay. The fast decay is independent of solute identity or concentration and is almost complete by 200 ps. We assign this fast component to diffusive geminate recombination of the dissociating pair (k_{recomb} in Figure 1). The slow decay component is always present, but its rate varies among solutes. We assign the slow decay to hydrogen abstraction by the surviving chlorine radicals with a rate constant k_{obs} that depends linearly on the concentration of the solute

$$k_{\text{obs}} = k_{\text{solvent}} + k_{\text{bi}}[\text{RH}] \quad (2)$$

where k_{solvent} is the rate constant for reaction with dichloromethane and k_{bi} is the rate constant for bimolecular reaction with the hydrogen-containing solute RH.

Subpicosecond time resolution allows us to observe directly very fast processes, such as the diffusion-controlled reactions and the diffusive geminate recombination of the fragments following photodissociation of dichloromethane. It also sets the stage for future studies of vibrationally mediated reactions that proceed on ultrafast time scales dictated by the short lifetimes of molecular vibrations in solution. Our solutes fall in four homologous series: straight-chain alkanes, cyclic alkanes, alcohols, and chlorinated alkanes. Within each series, structural differences among the solutes reveal interesting details about hydrogen abstraction reactions in solution.

II. Experimental Approach

The experimental arrangement requires an ultraviolet photolysis pulse to generate chlorine radicals and a tunable ultraviolet probe pulse to follow their evolution. We use a Coherent Vitesse oscillator to seed a Coherent Legend HE Ti:sapphire regenerative amplifier, which produces a 1-kHz train of 100-fs-duration (fwhm) pulses centered at 800 nm. A portion ($\sim 180 \mu\text{J}$) of the

amplified 800-nm light generates the photolysis pulse. We first double the 800-nm light by focusing it in a 0.3-mm type I β -barium borate (BBO) crystal ($\theta = 29^\circ$). We separate the resulting 400-nm light from residual 800-nm fundamental with a dichroic mirror, focus both beams, and recombine them in another 0.2-mm type I BBO crystal ($\theta = 42^\circ$) to produce $\sim 4 \mu\text{J}$ pulses centered at 266 nm by sum-frequency generation. Because these experiments do not require high photolysis power, we use neutral density filters to limit the photolysis pulses at the sample to about $0.75 \mu\text{J}$. To produce probe pulses, we use about $500 \mu\text{J}$ of the 800-nm light to pump a continuum-seeded, double-pass optical parametric amplifier (OPA) based on a $5 \times 5 \times 5 \text{ mm}^3$ type II BBO crystal ($\theta = 27^\circ$). The signal out of the OPA is conveniently tunable between 1120 and 1560 nm. We isolate the signal with a polarizer and quadruple it in two additional BBO crystals (1 mm, type I, $\theta = 22^\circ$, and 0.3 mm, type I, $\theta = 29^\circ$). The resulting probe pulses are tunable between 280 and 390 nm, with energies in excess of 100 nJ over the entire range. The photolysis and probe pulses are perpendicularly polarized to suppress coherent responses from the solvent.

A pair of quartz lenses ($f = 250$ and $f = 200$ mm) focus the photolysis and probe beams to diameters of ~ 100 and $\sim 50 \mu\text{m}$, respectively, in the sample where they cross at a small angle. Because the beams are not collinear, the resolution of our detection system is about 400 fs as measured by the two-photon solvent response. Two Si photodiodes monitor the probe light before and after the sample to account for shot-to-shot laser fluctuations. A chopper blocks every other photolysis pulse, and the probe intensity after the sample (normalized to probe intensity before the sample) with and without the photolysis pulse gives the transient pump-induced absorbance change. A Teflon gear pump circulates the sample through a 1-mm-thick Teflon cell with CaF_2 windows. A computer-controlled delay stage varies the time between pump and probe pulses. We average 4000 laser shots per point and achieve a noise level under 0.01 mOD.

The solvent in all experiments is HPLC-grade dichloromethane. The solutes are the highest purity available from Aldrich and do not require further purification. We take care to use solute concentrations that are low enough that reactions of secondary radicals are not important but are high enough that there is no significant depletion of solute during the experiment. Typical solute concentrations are less than 0.6 M.

III. Results

A. Neat Dichloromethane. Irradiation of neat dichloromethane with a 266-nm laser pulse produces a transient spectrum with a maximum near 330 nm, shown in Figure 2. A pump energy of about $0.75 \mu\text{J}$ per pulse results in a transient signal of 3–4 mOD at early delay times. The one-photon absorption of dichloromethane is very small at the photolysis wavelength, and a plot of the maximum transient signal versus photolysis energy is quadratic, consistent with a two-photon photodissociation. The band at 330 nm is a charge-transfer transition between a dichloromethane electron donor and a chlorine atom electron acceptor.²⁰ In the ground state, the chlorine atom is probably not truly free but is more likely in a loosely bound solvent–chlorine complex. Chateaufort measured reaction rates for chlorine atoms in several solvents²² and found that they are proportional to the ionization energy of the solvent. He proposed the presence of a weak chlorine–solvent complex with an association constant that depends on solvent ionization energy. Additional evidence for a bound ground-state complex

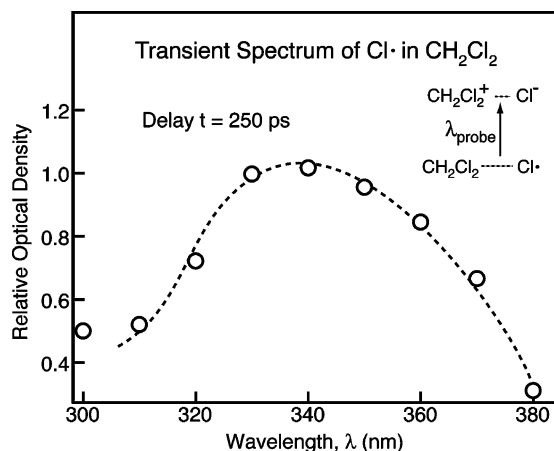


Figure 2. Transient spectrum at a delay $t = 250$ ps following photodissociation of CH_2Cl_2 . The dotted line is only a guideline.

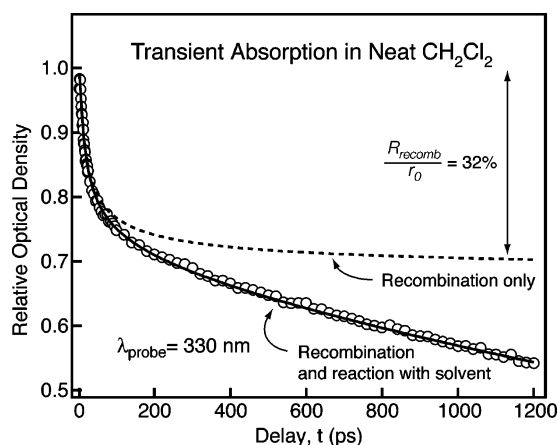


Figure 3. Transient response at $\lambda = 330$ nm following photodissociation of neat CH_2Cl_2 . The circles are experimental data. The solid line is the fit to the full model (eq 4), and the dotted line shows geminate recombination alone.

comes from Keiding and co-workers, who obtain a good fit of their experimental chlorine transient signal in aqueous solutions using a diffusion constant that is too small for an isolated Cl atom but is reasonable for a Cl–water complex.^{24,25} Elles et al. measured a transient spectrum of free Cl in dichloromethane that shifted to lower energy in the first few picoseconds, consistent with the presence of a weakly bound ground-state complex and a tightly bound excited-state charge-transfer complex.²⁶ As the chlorine radical thermalizes, the difference in the slopes of the ground-state and excited-state potentials produces a shift of the absorption wavelength. Thus, we assume that the free chlorine signal in our experiments is actually a weakly bound complex with the solvent.

The charge-transfer transition at 330 nm is a direct monitor of the chlorine population because no other species present in our experiment absorbs significantly between 300 and 400 nm. Figure 3 shows a typical normalized transient in neat CH_2Cl_2 . The signal rises to nearly its maximum value within the instrument response time. During the next 2 ps, it grows more slowly probably because of relaxation of the ground-state solvent–chlorine complex.²⁶ We limit our analysis to the behavior of the signal after 2 ps to focus on the reaction kinetics.

We fit the chlorine signal decay in neat dichloromethane using a variant of the Smoluchowski model.²⁷ In the model, the radical fragments of a dissociating pair equilibrate with the solvent at a distance r_0 and move randomly afterward with a relative diffusion constant D_{recomb} . Whenever two geminate fragments

approach each other to a distance R_{recomb} , they recombine without a barrier (k_{recomb} in Figure 1). The recombination gives a time-dependent Cl concentration of

$$[\text{Cl}](t) = [\text{Cl}](0) \left[1 - \frac{R_{\text{recomb}}}{r_0} \text{erfc} \left(\frac{r_0 - R_{\text{recomb}}}{\sqrt{4D_{\text{recomb}}t}} \right) \right] \quad (3)$$

The chlorine radicals that do not recombine go on to abstract a hydrogen atom from the solvent (k_{solvent} in Figure 1). Smoluchowski theory predicts a time-dependent reaction rate coefficient in cases where the early time concentration of the excess reactant is different from its steady-state concentration.²⁷ However, for neat CH_2Cl_2 , the change in concentration is negligible during the course of the reaction. Therefore, we ignore this time dependence and fit the slow component of the transient chlorine signal to a simple exponential decay with the pseudo-first-order rate constant k_{solvent} for hydrogen abstraction from dichloromethane. To compare neat solvent transients from different days, we normalize each transient to its maximum value and fit the *normalized* traces to the relation

$$S(t) = \left[1 - A \text{erfc} \left(\frac{B}{\sqrt{t}} \right) \right] \exp(-k_{\text{solvent}}t) \quad (4)$$

where

$$A \equiv \frac{R_{\text{recomb}}}{r_0} \quad B \equiv \frac{r_0 - R_{\text{recomb}}}{\sqrt{4D_{\text{recomb}}}}$$

The diffusion coefficient $D_{\text{recomb}} = 4.3 \text{ nm}^2 \text{ ns}^{-1}$ is the sum of the diffusion constants of the diffusing pair (a CH_2Cl radical and a Cl–solvent complex). We calculate each diffusion constant using the Stokes–Einstein expression, $D = k_B T / 6\pi\eta\alpha$, where η is the viscosity of neat dichloromethane and α is the radius of the diffusing particle.²⁸ We fit eight different neat solvent transients to generate statistics on the fit parameters shown in Table 1. Knowing the diffusion constant allows us to calculate R_{recomb} and r_0 from the values of A and B .

B. Dichloromethane Solutions. Upon addition of a hydrogen-containing solute RH, the slow component of the transient chlorine signal decay becomes faster due to the new reactive pathway, $\text{Cl}\cdot + \text{RH} \rightarrow \text{R}\cdot + \text{HCl}$. Immediately after the formation of Cl radicals, the solute concentration around them is higher than in the steady state that characterizes the bulk reaction.²⁷ Therefore, bimolecular rate coefficients for reactions with solute are time-dependent in accordance with Smoluchowski theory. The time-dependent Cl concentration in a diffusion-controlled bimolecular reaction is

$$[\text{Cl}](t) = [\text{Cl}](0) \exp \left\{ -4\pi R_{\text{rxn}} D_{\text{rxn}} C_{\text{solute}} \left(1 + \frac{2R_{\text{rxn}}}{\sqrt{\pi D_{\text{rxn}} t}} \right) t \right\} \quad (5)$$

where R_{rxn} is the reaction radius, D_{rxn} is the sum of diffusion constants of reactants (solute RH and Cl–solvent complex), and C_{solute} is the solute concentration. At early times (< 0.2 ns), the second term in the exponential is large and produces significant deviations from single-exponential decay. However, at long times, corresponding to bulk reactions, this equation simplifies to a single-exponential decay with the steady-state rate constant

$$k_{\text{bi}}(t)|_{t \rightarrow \infty} = 4\pi R_{\text{rxn}} D_{\text{rxn}} \left(1 + \frac{2R_{\text{rxn}}}{\sqrt{\pi D_{\text{rxn}} t}} \right) \Big|_{t \rightarrow \infty} = 4\pi R_{\text{rxn}} D_{\text{rxn}} \quad (6)$$

TABLE 1: Fit Parameters and Rate Constants for All Data

		adjustable parameters		calculated values		k_{bi} ($10^7 \text{ M}^{-1} \text{ s}^{-1}$)	
neat CH_2Cl_2		A	0.32 ± 0.01	r_0 (nm)	0.50 ± 0.05	this work	1.36 ± 0.06
		B ($\text{ns}^{-1/2}$)	0.082 ± 0.005	R_{recomb} (nm)	0.16 ± 0.02	literature ^a	0.9 ± 0.2
		k_{solvent} (ns^{-1})	0.21 ± 0.01				
		fixed parameters ^b		adjustable parameters		k_{bi} ($10^9 \text{ M}^{-1} \text{ s}^{-1}$)	
solute	C_{solute} (M)	D_{rxn} ($\text{nm}^2 \text{ ns}^{-1}$)	R_{rxn} (nm)	this work	literature ^c		
pentane	0.05–0.3	2.84	0.43 ± 0.03	9.3 ± 0.7			
hexane	0.05–0.3	2.78	0.49 ± 0.05	10.4 ± 1.0			
heptane	0.05–0.3	2.73	0.53 ± 0.04	10.8 ± 0.8			
cyclopentane	0.05–0.3	2.95	0.45 ± 0.04	10.1 ± 0.9			
cyclohexane	0.05–0.3	2.87	0.52 ± 0.04	11.4 ± 0.8	5.4 (11.7 ± 2.3) ^d		
cycloheptane	0.05–0.3	2.82	0.55 ± 0.05	11.8 ± 1.2			
methanol	0.1–0.6	3.46	0.20 ± 0.04	5.2 ± 1.1	2.7 (5.9) ^e		
ethanol	0.05–0.3	3.22	0.29 ± 0.09	7.1 ± 2.2	3.3 (7.3) ^e		
1-propanol	0.05–0.3	3.07	0.33 ± 0.06	7.7 ± 1.5	5.6 (12.3) ^e		
2-propanol	0.05–0.3	3.06	0.27 ± 0.05	6.3 ± 1.3	3.7 (8.1) ^e		
1-butanol	0.05–0.3	2.96	0.40 ± 0.06	9.0 ± 1.4	7.0 (15.4) ^e		
cyclohexyl chloride	0.1–0.6	2.83	0.30 ± 0.03	6.5 ± 0.6	2.3 (7.2 ± 1.6) ^f		
1-chlorobutane	0.2–0.6	2.89	0.21 ± 0.05	4.5 ± 1.1			
2-chlorobutane	0.4–1.8	2.88	0.07 ± 0.02	1.4 ± 0.4			
1,2-dichlorobutane	0.4–1.7	2.85	0.05 ± 0.02	1.0 ± 0.5			
1,4-dichlorobutane	0.4–1.8	2.87	0.04 ± 0.01	0.9 ± 0.3			

^a Reference 17. ^b Fixed parameters also include the solvent contribution $S(t)$ determined by fits to neat CH_2Cl_2 . ^c The value in parentheses is corrected for solvent viscosity, if different from that of CH_2Cl_2 . ^d Reference 23. ^e Reference 36. ^f Reference 26.

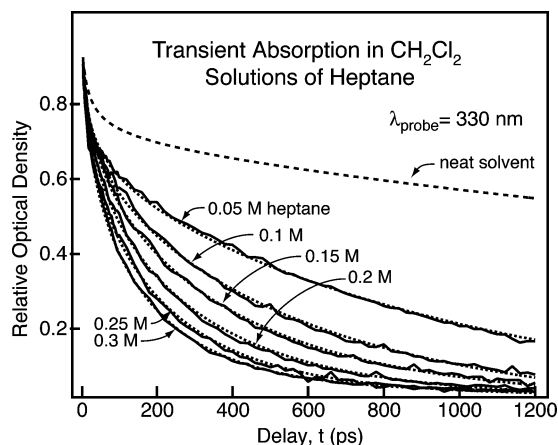


Figure 4. Normalized transient response at $\lambda = 330 \text{ nm}$ in solutions with various concentrations of *n*-heptane. The solid lines are experimental data, and the dotted lines are simultaneous fits to eq 7. The dashed line is the fit to the transient response from neat solvent, shown in Figure 3.

The parameter R_{rxn} is an “effective reaction radius” at which a reaction proceeds with unit probability, and for activation-controlled reactions, R_{rxn} is smaller than the sum of the reactant radii because not all encounters between reactants lead to products.^{27,29}

Figure 4 shows the normalized transients for six different concentrations of *n*-heptane in dichloromethane along with the fits from the Smoluchowski theory. When fitting the transients that contain reactions with the *solute*, we include the *solvent* contribution as a parameter $S(t)$ with time dependence determined from neat dichloromethane measurements. The complete fit is to the equation

$$\frac{[\text{Cl}](t)^{(n)}}{[\text{Cl}](0)} = S(t) \exp \left\{ -4\pi R_{\text{rxn}} D_{\text{rxn}} C_{\text{solute}}^{(n)} \left(1 + \frac{2R_{\text{rxn}}}{\sqrt{\pi D_{\text{rxn}} t}} \right) t \right\} + S_{\infty}^{(n)} \quad (7)$$

where S_{∞} is a long-time offset and the superscript (n) denotes different concentrations of a particular solute. The fixed parameters are $S(t)$ from eq 4, D_{rxn} from the Stokes–Einstein equation, and C_{solute} . We fit all concentrations simultaneously, using global values for $S(t)$, R_{rxn} , and D_{rxn} but letting S_{∞} vary from trace to trace. We calculate the steady-state bimolecular reaction constant k_{bi} using eq 6. A typical value for the offset is less than 10% of the maximum signal, and its effect on the fit is minimal. In particular, the bimolecular reaction constants k_{bi} for all solutes do not change outside of their error limits if we remove the offset altogether. Table 1 gives the fit parameters for all solvents along with the values for k_{bi} (all of the uncertainties are one standard deviation).

The fits show that the long-time offset S_{∞} increases monotonically with increasing solute concentration. The magnitude of this increase depends on the identity of the solute, being smallest in alcohols and largest in chlorinated alkanes. The offset is likely absorption by a solute radical $\text{R}\bullet$ or its derivative, $\text{RO}_2\bullet$, formed by reaction with O_2 in oxygen-containing solutions,^{17,30,31} since many organic radicals or their derivative peroxy radicals absorb at wavelengths longer than 300 nm.^{30–32} Because the solute RH competes with the solvent for chlorine atoms, the final concentration of $\text{R}\bullet$ depends on the fraction of chlorine atoms that react with RH compared to that reacting with the solvent dichloromethane

$$[\text{R}\bullet]_{\infty} = [\text{Cl}\bullet]_0 \frac{k_{bi}[\text{RH}]}{k_{bi}[\text{RH}] + k_{\text{solvent}}} \quad (8)$$

The final number of solute radicals increases (although *not linearly*) with increasing solute concentration. To test this model, we measure the photolysis-induced absorption for various concentrations of methanol, cyclohexane, cyclohexyl chloride, and 1,4-dichlorobutane at a delay of 15 ns, when the chlorine decay is essentially complete. We observe the behavior of the offset predicted by eq 8, including the nonlinear dependence on solute concentration. A similar measurement for cyclohexyl chloride dissolved in CCl_4 shows no increase in the offset at

higher solute concentrations because CCl_4 does not react with chlorine in competition with the solute.

IV. Discussion

A. Neat Dichloromethane. The decay of chlorine atoms in neat dichloromethane has two components, diffusive geminate recombination and hydrogen abstraction. As shown in Figure 3, recombination dominates the transient signal at early times (≤ 200 ps). We can compare the values for the recombination parameters D_{recomb} , R_{recomb} , and r_0 to those from Keiding and co-workers, who investigated the recombination dynamics following photolysis of HOCl in water at wavelengths corresponding to excess energies between 1.5 and 3 eV.²⁵ Using the value of $D_{\text{recomb}} = 3 \text{ nm}^2 \text{ ns}^{-1}$ from Parsons et al.³³ and $R_{\text{recomb}} \approx 0.35 \text{ nm}$, they found that the initial separation of the fragments is in the range of 0.4–0.6 nm and varies linearly with the excess photolysis energy. In contrast, we calculate a slightly higher value of $D_{\text{recomb}} = 4.3 \text{ nm}^2 \text{ ns}^{-1}$, consistent with dichloromethane being less viscous than water. Our fits of the recombination of CH_2Cl and chlorine yield a value of $R_{\text{recomb}} = (0.16 \pm 0.02) \text{ nm}$, about 50% lower than that of Keiding et al., despite CH_2Cl being larger than the OH radical. However, they estimate R_{recomb} from the point on a gas-phase collinear potential surface³⁴ where the fragments experience an attractive force equal to kT . Such an assumption is valid only for the most favorable approach geometry and ignores steric effects. Our value of R_{recomb} is about 4 times smaller than the physical radii of the recombining fragments, reflecting the possibility of unfavorable collision orientations.

In comparison to the aqueous HOCl experiment of Keiding and co-workers, the two-photon dissociation of dichloromethane at 266 nm in our experiment leaves much more excess energy in the resulting fragments (about 5.8 eV, calculated using a gas-phase C–Cl bond strength of 3.5 eV³⁵ and neglecting solvation effects). In addition, dichloromethane is only about one-half as viscous as water, and therefore it is surprising that our value of $r_0 = (0.50 \pm 0.04) \text{ nm}$ is about the same as that of Keiding et al. However, the photolysis of CH_2Cl_2 may occur after fast internal conversion with some of the excess energy dissipated by the solvent or deposited in the internal degrees of freedom of the CH_2Cl radical. In contrast, in the photolysis of HOCl all of the excess dissociation energy goes into kinetic energy of the fragments.²⁵ In the analysis based on Smoluchowski theory, the parameters R_{recomb} and r_0 are potentially correlated because their ratio, R_{recomb}/r_0 , determines the asymptotic fraction of chlorine atoms that recombine with their partner radical.^{27,36} Therefore, in fitting the chlorine transients, the value of r_0 depends on the arbitrarily chosen R_{recomb} , and our low value for the initial separation of the fragments is consistent with the smaller recombination radius. Despite the physical ambiguity of R_{recomb} , the fit is quite robust and gives the recombination yield of $R_{\text{recomb}}/r_0 = 0.32 \pm 0.01$.

The chlorine atoms that survive diffusive geminate recombination decay in $(4.7 \pm 0.2) \text{ ns}$. Because the concentration of neat dichloromethane is 15.6 M, the corresponding bimolecular rate constant for hydrogen abstraction by chlorine is $(1.36 \pm 0.07) \times 10^7 \text{ M}^{-1} \text{ s}^{-1}$. It is larger than two other experimental values of $0.6 \times 10^7 \text{ M}^{-1} \text{ s}^{-1}$ obtained by Emmi et al.¹⁸ (which they give as a lower limit) and $(0.9 \pm 0.2) \times 10^7 \text{ M}^{-1} \text{ s}^{-1}$ by Alfassi et al.¹⁷ However, multiple secondary reactions make their experiments more complicated to interpret, and they do not observe the chlorine radical directly but rather infer its decay rate from competing processes. Avoiding secondary reactions is one of the advantages of using ultrafast time resolution to observe reactions in solution.

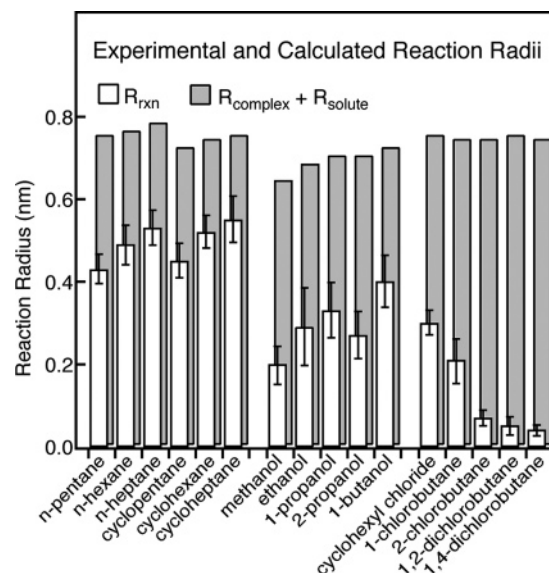


Figure 5. Comparison of experimental reaction radii, R_{rxn} , defined as the radius of approach at which reactants form products with unit probability, to the physical size of the pair, $R_{\text{pair}} = R_{\text{complex}} + R_{\text{solute}}$, calculated from the molar volumes of the reactants.

B. Dichloromethane Solutions. The most important parameters extracted from the fits are the effective reaction radii R_{rxn} , shown in Table 1. A discrepancy between R_{rxn} and the physical size of the reactants indicates the presence of a long-range interaction potential.^{27,29} For example, a reaction radius that is too small suggests that the reaction proceeds over a barrier. Conversely, a reaction radius that is too large implies an attractive interaction between the reactants. Figure 5 shows the reaction radii for all solutes we studied along with the physical size of the reacting pair, $R_{\text{pair}} = R_{\text{complex}} + R_{\text{solute}}$, calculated using the molar volumes of the reacting particles and the assumption that they are spherical. We calculate the size of a chlorine–dichloromethane complex by adding together radii of a chlorine atom and a solvent molecule. This approximate value of R_{pair} is a guide in interpreting our results.

The alkanes (*n*-pentane, *n*-hexane, *n*-heptane, and their cyclic analogues) have the largest reaction radii, and their values are the closest to the physical size of the reactants. In fact, neither size nor shape (comparing linear and cyclic alkanes) seems to have a large effect on the reaction radii. This result is consistent with the reactions being diffusion-limited and with the difference between R_{rxn} and R_{pair} likely arising from steric effects of the Cl–solvent complex. We expect that there is a range of orientations where the chlorine–solvent complex presents the wrong side to the solute molecule, making hydrogen abstraction impossible. Additional evidence for the alkane reactions being diffusion-limited comes from the work of Raftery et al.²³ who measured a bimolecular rate constant for hydrogen abstraction from neat cyclohexane that is about 50% lower than ours. However, the Smoluchowski reaction rate constant is proportional to the diffusion constant D_{rxn} , which is in turn inversely proportional to the solvent viscosity. Correcting for the difference in viscosity between cyclohexane and dichloromethane brings the two rates into good agreement, as expected for a diffusion-limited reaction.

Alcohols have uniformly smaller reaction radii than alkanes, and within the series from methanol to butanol, the variation of R_{rxn} is larger. This observation suggests that the reaction rate is not purely diffusion-limited and that activation energy plays a role. For example, the reaction radius decreases in going from 1-propanol to 2-propanol, implying site specificity in the

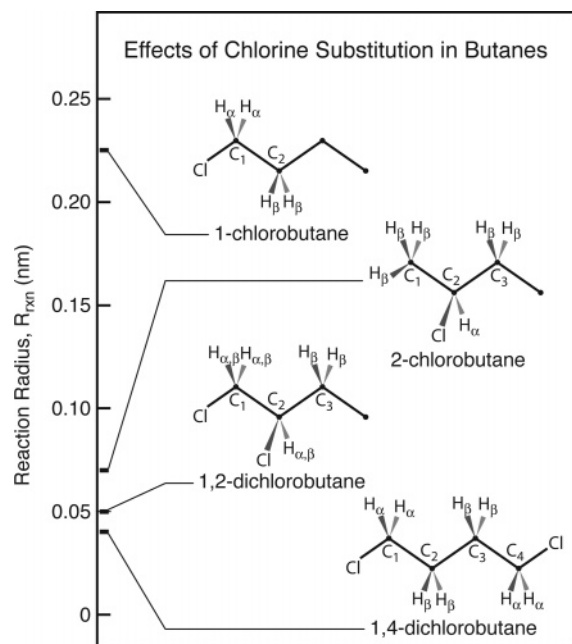


Figure 6. Effects of chlorine substitution on the reactivities of the four chlorinated butanes. For each molecule, the affected carbon and hydrogen atoms are explicitly labeled. For hydrogen atoms, the labels include the strength of the deactivating effect, determined by the position (α , β) relative to the chlorine substituent (also labeled).

chlorine atom attack that is consistent with activation-controlled reactions. In the gas phase, chlorine reactions are about 4 times faster with secondary hydrogens than with primary hydrogens.^{5,6} Because 1-propanol has more secondary hydrogens and fewer primary hydrogens than 2-propanol, its overall reactivity is higher, similar to the gas phase. We can compare our reaction rates to those measured by Sumiyoshi et al. in aqueous solution.³⁷ Their rates are 25–50% smaller than ours, but the qualitative trends are the same, including the difference between the two propanol isomers. There are two reasons for the discrepancy in absolute values of the reaction rates. First, the higher viscosity of water as compared to CH_2Cl_2 slows down the almost diffusion-controlled reactions. Second, their rates reflect the reactivity of the chlorine–water complex, different from that of the chlorine–dichloromethane complex.²²

The most striking comparison is for the chlorinated alkanes. In the gas-phase, chlorine substitution deactivates C–H bonds, especially for hydrogens in β -positions,^{12,14,16} and our results follow the same qualitative trend. Cyclohexyl chloride has a much smaller reaction radius than cyclohexane, despite having a similar physical size. The effect on chlorinated butanes is even more dramatic. There are no data on hydrogen abstraction from *n*-butane in solution, but extrapolating our results for the other straight-chain alkanes gives a reaction radius of about 0.4 nm, much larger than the halogenated butane species in our study. Figure 6 shows the effects of chlorine substitution on reaction radii of the four chlorinated butanes. Of these, 1-chlorobutane has the largest reaction radius because the halogen substituent deactivates only the C_1 and C_2 hydrogens. In 2-chlorobutane, the chlorine substituent affects the position C_1 through C_3 in the four-carbon backbone, leading to a much smaller R_{rxn} . In 1,2-dichlorobutane, two halogens affect three of the four carbon positions (with the C_1 and C_2 hydrogens affected by the presence of both chlorines), leading to a still smaller R_{rxn} . Finally, in 1,4-dichlorobutane all of the C–H bonds are affected, and the reaction radius is the smallest of all the solutes in this study.

TABLE 2: Comparison of Experimental Rate Constants with Those from Structure–Activity Relationships

SAR parameters			
group	weighting factor	type of hydrogen	k_g ($10^9 \text{ M}^{-1} \text{ s}^{-1}$) ^a
–Cl	0.4 ^b	primary	0.61 ^b
–CH ₃	5.1 ^b	secondary	1.52 ^b
–CH ₂ Cl	0.76 ^b	tertiary	1.11 ^b
–CH ₂ –R	30.3 ^b		
–CHCl–R	4.5		

solute	relative rate constant k_{bi}	
	this study	SAR prediction
cyclohexane ^c	1.7	1.7
cyclohexyl chloride ^c	1	1
<i>n</i> -butane ^d	8 ^e	7.4
1-chlorobutane ^d	4.4	4.5
2-chlorobutane ^d	1.4	1.4
1,2-dichlorobutane ^d	1	1
1,4-dichlorobutane ^d	0.9	1.5

^a k_g is the gas-phase hydrogen abstraction rate on a per atom basis. ^b Reference 15. ^c The rate constants are normalized to that of cyclohexyl chloride. ^d The rate constants are normalized to that of 1,2-dichlorobutane. ^e This value is extrapolated from rate constants for pentane, hexane, and heptane.

It is interesting that gas-phase trends concerning the influence of substituents survive in liquid-phase reactions. Solvent interactions, even in a weakly interacting bath such as dichloromethane, can perturb a reaction considerably. Diffusion and caging change the ways in which reactant species approach each other as well as the time they spend near each other. These effects are apparent in alkanes and alcohols, all of which have reaction rate constants that are 10 to 20 times smaller in solution than in the gas phase. The chlorinated species, however, are much more sensitive to the details of the reactive potential surface because they have a barrier to reaction. It seems that solvation by dichloromethane does not change the transition-state region of the reactive potential surface drastically.

C. Comparison with Structure–Activity Relationships. Our results allow us to apply the structure–activity relationships (SAR) to activation-controlled reactions of chlorinated butanes and cyclohexyl chloride in solution. We base our analysis on parameters reported by Senkan and Quam in an extensive gas-phase study of methane and ethane derivatives, where all the neighboring groups are, at most, one-carbon moieties.¹⁶ Because our solutes are larger and have a greater variety of neighboring groups, we extend their method by making two assumptions. We assume that the first carbon in a neighboring group determines the influence of that group on adjacent C–H bonds. For example, all neighboring groups that have the form $-\text{CH}_2-\text{R}$ have the same weighting factor regardless of the identity of R. Aschman et al. achieve good agreement with experimental data by making the same assumption in their analysis of chlorine atom reactions with saturated alkanes.¹⁵ There are five classes of neighboring groups in our solutes ($-\text{Cl}$, $-\text{CH}_3$, $-\text{CH}_2\text{Cl}$, $-\text{CH}_2-\text{R}$, and $-\text{CHCl}-\text{R}'$), with the weighting factors for only the first four of these available from the literature.¹⁶ We further assume that a chlorine substituent in the β position has an effect that is independent of the rest of the neighboring group. Senkan and Quam list a weighting factor of 0.76 for the $-\text{CH}_2\text{Cl}$ group, 6.7 times smaller than that for the methyl group (5.1). By analogy, we assign a weighting factor of 4.5 to the $-\text{CHCl}-\text{R}'$ group, which is 6.7 times smaller than the value of 30.3 for the $-\text{CH}_2-\text{R}$ group. Table 2 lists all of the weighting factors along with the reactivities for primary, secondary, and tertiary hydrogen atoms.

We calculate the SAR rate constants according to eq 1 and compare the results to our experimental rate constants for cyclohexane, cyclohexyl chloride, *n*-butane, and chlorinated butanes. A direct comparison of the magnitudes of the rate constants is not useful because the SAR analysis uses rate constants k_{pri} , k_{sec} , and k_{ter} for reactions in the gas phase, which are much faster than those in solution. Instead, we compare the *relative* experimental rate constants to those predicted by the structure–activity relationships. Table 2 shows the rate constant for cyclohexane relative to that of cyclohexyl chloride and for butanes relative to that of 1,2-dichlorobutane. The experimental k_{bi} for *n*-butane is an extrapolation of our values for the other straight-chain alkanes. The agreement between SAR predictions and experiment is excellent. The only significant deviation is a 65% overestimate in the rate constant of 1,4-dichlorobutane, which is slightly outside of our experimental error limits. Our results suggest that the structure–activity relationships are useful for predicting the relative rates of activation-controlled reactions in weakly interacting solvents such as dichloromethane.

V. Summary

We generate reactive chlorine atoms in solution by two-photon photodissociation of the solvent dichloromethane and monitor the nascent chlorine radical population via a charge-transfer transition. The chlorine atoms that do not immediately recombine with their partner radicals escape the solvent cage within the instrument response time. The chlorine signal rises slowly for about 2 ps, probably reflecting the relaxation of a weak chlorine–solvent complex, and decays with two distinct components, a fast diffusive geminate recombination of the dissociated fragments and a slower hydrogen abstraction reaction.

We fit the fast component of the chlorine decay to a diffusive geminate recombination model based on pair survival probability. Geminate recombination is complete within about 200 ps and accounts for the loss of about one-third of the solvated chlorine atoms. The other two-thirds of the chlorine atoms go on to abstract a hydrogen atom. Hydrogen abstraction from the solvent occurs with a lifetime of about 5 ns, in good agreement with literature values. Upon the addition of solutes, the chlorine decay becomes faster, and the signal returns to baseline within 1 ns, depending on the solute concentration. We study four different classes of solutes: straight-chain alkanes, cyclic alkanes, alcohols, and chlorinated alkanes. The hydrogen abstraction reactions from alkanes are diffusion-limited. Pentane, hexane, heptane, and their cyclic analogues have similar rate constants that are about 20 times slower than those in the gas phase. Reactions of alcohols show a wider range of rate constants. Two propanol isomers have rate constants that differ by about 20%, suggesting that the reactions are partially activation-controlled. The chlorinated alkane species are also activation-controlled, with rate constants that depend strongly on the molecular structure. We compare our experimental results to predictions of the gas-phase structure–activity relationships and find excellent agreement in the relative rates. Our results

suggest that SAR is a useful means of estimating the relative reactivity of organic molecules in weakly interacting solvents.

Acknowledgment. We are grateful to Jocelyn Cox and George Barnes for many helpful discussions. A.C.C. thanks the National Science Foundation for a predoctoral fellowship. The National Science Foundation supports this work.

References and Notes

- (1) Farman, J. C.; Gardiner, B. G.; Shanklin, J. D. *Nature* **1985**, *315*, 207.
- (2) Finlayson-Pitts, B. J. *Res. Chem. Int.* **1993**, *19*, 235.
- (3) Molina, M. J.; Rowland, F. S. *Nature* **1974**, *249*, 810.
- (4) Singh, H. B.; Kasting, J. F. *J. Atmos. Chem.* **1988**, *7*, 261.
- (5) Tyndall, G. S.; Orlando, J. J.; Wallington, T. J.; Dill, M.; Kaiser, E. W. *Int. J. Chem. Kinet.* **1997**, *29*, 43.
- (6) Sarzynski, D.; Sztuba, B. *Int. J. Chem. Kinet.* **2002**, *34*, 651.
- (7) Lewis, R. S.; Sander, S. P.; Wagner, S.; Watson, R. T. *J. Phys. Chem.* **1980**, *84*, 2009.
- (8) Tyndall, G. S.; Orlando, J. J.; Kegley-Owen, C. S.; Wallington, T. J.; Hurley, M. D. *Int. J. Chem. Kinet.* **1999**, *31*, 776.
- (9) Thevenet, R.; Mellouki, A.; Le Bras, G. *Int. J. Chem. Kinet.* **2000**, *32*, 676.
- (10) Mcloughlin, P.; Kane, R.; Shanahan, I. *Int. J. Chem. Kinet.* **1993**, *25*, 137.
- (11) Wine, P. H.; Semmes, D. H. *J. Phys. Chem.* **1983**, *87*, 3572.
- (12) Dobis, O.; Benson, S. W. *J. Phys. Chem. A* **2000**, *104*, 5503.
- (13) Miyokawa, K.; Tschuikowroux, E. *J. Phys. Chem.* **1990**, *94*, 715.
- (14) Kelly, C. C.; Wijnen, M. H. J. *J. Phys. Chem.* **1969**, *73*, 2447.
- (15) Aschmann, S. M.; Atkinson, R. *Int. J. Chem. Kinet.* **1995**, *27*, 613.
- (16) Senkan, S. M.; Quam, D. J. *J. Phys. Chem.* **1992**, *96*, 10837.
- (17) Alfassi, Z. B.; Mosseri, S.; Neta, P. *J. Phys. Chem.* **1989**, *93*, 1380.
- (18) Emmi, S. S.; Beggiato, G.; Casalboremiceli, G. *Radiat. Phys. Chem.* **1989**, *33*, 29.
- (19) Forgeteg, S.; Berces, T. *J. Photochem. Photobiol., A* **1993**, *73*, 187.
- (20) Chateaufneuf, J. E. *Chem. Phys. Lett.* **1989**, *164*, 577.
- (21) Chateaufneuf, J. E. *J. Am. Chem. Soc.* **1990**, *112*, 442.
- (22) Chateaufneuf, J. E. *J. Org. Chem.* **1999**, *64*, 1054.
- (23) Raftery, D.; Iannone, M.; Phillips, C. M.; Hochstrasser, R. M. *Chem. Phys. Lett.* **1993**, *201*, 513.
- (24) Madsen, D.; Thomsen, C. L.; Poulsen, J. A.; Jensen, S. J. K.; Thogersen, J.; Keiding, S. R.; Krissinel, E. B. *J. Phys. Chem. A* **2003**, *107*, 3606.
- (25) Thomsen, C. L.; Madsen, D.; Poulsen, J. A.; Thogersen, J.; Jensen, S. J. K.; Keiding, S. R. *J. Chem. Phys.* **2001**, *115*, 9361.
- (26) Elles, C. G.; Cox, M. J.; Barnes, G. L.; Crim, F. F. *J. Phys. Chem. A* **2004**, *108*, 10973.
- (27) Rice, S. A. *Diffusion-Limited Reactions*; Comprehensive Chemical Kinetics 25; Elsevier: New York, 1985.
- (28) We assume the radius of a CH₂Cl radical to be equal to 0.18 nm, the sum of the radii of a chlorine and a carbon atom. To estimate the radius of the Cl–solvent complex, we add the radii of a chlorine atom (0.1 nm) and the solvent molecule (0.29 nm, calculated using the molar volume of dichloromethane).
- (29) Collins, F. C.; Kimball, G. E. *J. Colloid Sci.* **1949**, *4*, 425.
- (30) Langer, S.; Ljungstrom, E.; Sehested, J.; Nielsen, O. J. *Chem. Phys. Lett.* **1994**, *226*, 165.
- (31) Platz, J.; Sehested, J.; Nielsen, O. J.; Wallington, T. J. *J. Phys. Chem. A* **1999**, *103*, 2688.
- (32) Joens, J. A. *J. Phys. Chem.* **1994**, *98*, 1394.
- (33) Parsons, R. *Handbook of Electrochemical Constants*; Butterworth: London, 1959.
- (34) Peterson, K. A.; Skokov, S.; Bowman, J. M. *J. Chem. Phys.* **1999**, *111*, 7446.
- (35) Tschuikow-Roux, E.; Paddison, S. *Int. J. Chem. Kinet.* **1987**, *19*, 15.
- (36) Tachiya, M. *Radiat. Phys. Chem.* **1983**, *21*, 167.
- (37) Sumiyoshi, T.; Miura, K.; Hagiwara, H.; Katayama, M. *Chem. Lett.* **1987**, 1429.